An input-to-state stability approach to verify almost global stability of a synchronous-machine- infinite-bus system

Johannes Schiffer, Denis Efimov, Romeo Ortega, Nikita Barabanov

PHILOSOPHICAL TRANSACTIONS A

rsta.royalsocietypublishing.org

Research

Article submitted to journal

Subject Areas:
Power systems, control systems, nonlinear dynamics

Keywords:
Power system dynamics, power system stability, nonlinear control systems, input-to-state stability

Author for correspondence:
Johannes Schiffer
e-mail: j.schiffer@leeds.ac.uk

An input-to-state stability approach to verify almost global stability of a synchronous-machine-infinite-bus system

Johannes Schiffer[1], Denis Efimov[2,5], Romeo Ortega[3] and Nikita Barabanov[4,5]

[1]School of Electronic and Electrical Engineering, University of Leeds, Leeds LS2 9JT, UK
[2]Non-A team@INRIA, Parc Scientifique de la Haute Borne, 40 avenue Halley, 59650 Villeneuve d'Ascq, France, with LAGIS UMR 8219, Ecole Centrale de Lille, Avenue Paul Langevin, 59651 Villeneuve d'Ascq, France
[3]Laboratoire des Signaux et Systémes, École Supérieure d'Electricité (SUPELEC), Gif-sur-Yvette 91192, France
[4]Department of Mathematics, North Dakota State University, Fargo, ND 58102, USA
[5]Department of Control Systems and Informatics, University ITMO, 49 Avenue Kronverkskiy, 197101 Saint Petersburg, Russia

Conditions for almost global stability of an operating point of a realistic model of a synchronous generator with constant field current connected to an infinite bus are derived. The analysis is conducted by employing the recently proposed concept of input-to-state stability (ISS)-Leonov functions, which is an extension of the powerful cell structure principle developed by Leonov and Noldus to the ISS framework. Compared to the original ideas of Leonov and Noldus, the ISS-Leonov approach has the advantage of providing additional robustness guarantees. The efficiency of the derived sufficient conditions is illustrated via numerical experiments.

THE ROYAL SOCIETY PUBLISHING

1. Introduction

(a) Motivating challenges

Modern industrialized societies heavily rely on the use and steady supply of electric energy. Therefore, it is of paramount importance to guarantee the stable, reliable and efficient operation of our power systems. However, the latter are bulk, complex and highly nonlinear systems that are continuously subjected to a large variety of disturbances and contingencies [1,21]. Hence, ensuring the stability of a power system is a daunting task, which has been at the core of power system operation since its early days in the 1920s [27,28]—see [21, Chapter 1] for a review of the research history on power system stability analysis.

Over the past decades, the complexity of this task has continuously exacerbated due to the penetration of large shares of volatile renewable energy sources. While this is a very desirable development from environmental and societal factors, the reliable and efficient integration of high amounts of renewable energy sources represents a major technical challenge for the operation of power systems [11,37]. In particular, the increasing presence of such units results in power systems more frequently operating closer to their security margins [11,37]. As a consequence, the problem of power system stability can be expected to become even more relevant in the coming years. This makes it important to derive easily and quickly verifiable analytic conditions for stability, which is the topic addressed in the present work.

A further motivation for our work is the fact that—despite the rich and extensive literature on power system stability—even today many basic questions remain open. This applies to the analysis of vast networks, but also to individual network components and is explained by the complexity of their dynamics. Thus, researchers and practitioners alike are forced to invoke several assumptions simplifying the mathematical tasks of stability analysis and control design. Amongst the most prevalent assumptions are neglecting fast dynamics [29,33,35], constant voltage amplitudes and small frequency variations [21, Chapter 11], [35]. Invoking such assumptions allows to derive reduced-order synchronous generator (SG) models [21, Chapter 11] and employ algebraic line models [29,33,35], which significantly simplifies the analysis. Unfortunately, most of the employed assumptions are not physically justifiable in generic operation scenarios. A paramount example for this is the common approximation of the motion of the machine rotor, *i.e.*, the swing equation, in terms of mechanical and electrical power instead of their corresponding torques. However, as this approximation is only valid for small frequency variations around the nominal frequency, it is not an adequate representation of the true physical system when the latter is subjected to large disturbances [1,16,21]; see also the discussions in [7,8,12,32]. In summary, a main limitation of current power system stability analysis methods is that they are based on reduced-order models only valid within a limited range of operating conditions. A direct consequence of this is that any stability assessment relying on such reduced-order models may lead to erroneous predictions [7,32], which—in the worst case—could lead to a blackout.

(b) Existing literature and contributions

In the present work, we perform a *global* stability analysis of a classical and very well known system called the single-machine-infinite-bus (SMIB) model [1,16]. Thereby, the main distinction to existing results [1,21] is that, motivated by the above discussion, we consider a fourth-order nonlinear SG model derived from first principles—instead of the usual simplified SG models. A thorough analysis and understanding of the SMIB scenario is a fundamental step in the development of a systematic mathematical framework for the analysis of more complex power system dynamics under less restrictive and more realistic assumptions as in [8,12] or in the classical literature [1,16,21]. Furthermore, the insights that can be gained from our analysis can provide valuable practical conclusions for the design, control and operation of SGs as well as

for the implementation of an emerging strand of control concepts that aim at operating grid-connected inverters such that they mimic the dynamics of conventional SGs [6,34,39]. The latter objective also has motivated the related works [23,24]. The analysis in [23] proceeds along the classical lines of constructing an integro–differential equation resembling the forced pendulum equation and, subsequently, showing that the SGIB system is almost globally asymptotically stable if and only if an equilibrium of that forced pendulum equation is almost globally asymptotically stable. In [24] the same authors provide slightly simpler conditions for stability resulting from verifying if a real-valued nonlinear map defined on a finite interval is a contraction. But, as stated in [24], these conditions are hard to verify analytically. Furthermore, and perhaps more importantly, the geometric tools employed to establish the results in [23,24], don't seem to be applicable to a multi–machine power system. In [8] a scenario similar to that of the SMIB system is analyzed. However, the analysis in [8] is conducted under very stringent assumptions on the specific form of the infinite bus voltage, as well as the steady-state values of the mechanical torque. A nonlinear analysis of the SMIB system is also conducted in [36], yet using a power rather than a torque balance in the swing equation and neglecting the stator dynamics. Then the SMIB model reduces to a nonlinear forced pendulum, as also studied in [9,10].

To achieve our main objective, *i.e.* the provision of sufficient conditions for almost global stability of the attractive equilibrium set of the SMIB system, we employ the recently developed framework of input-to-state (ISS) stability for *periodic* systems with multiple invariant sets [9]. Therein, the ISS approach from [2,3] is combined with the cell structure principle developed in [13,18,19,26,38] to derive necessary and sufficient conditions for ISS of periodic systems. This permits to *relax* the usual sign definiteness requirements on the Lyapunov function and its time-derivative by exploiting the periodicity of the system. This relaxation is essential to establish the main result of the present paper. More precisely, the main contributions of the paper are three-fold.

- Provide a sufficient condition for ISS of the equilibrium set of the SMIB system.
- By using this result, establish almost global asymptotic stability of the attractive equilibrium set of the SMIB system, *i.e.*, we show that for all initial conditions, except a set of measure zero, the solutions of the SMIB system asymptotically converge to an asymptotically stable equilibrium point.
- Illustrate the efficiency of the proposed conditions numerically via a benchmark example taken from [1, Table D.2].

Differently from our previous related work [4,5], in which LaSalle's invariance principle is employed, the present ISS-based approach has the advantage of providing additional robustness guarantees with respect to exogeneous inputs. Both properties—stability and robustness—are highly desirable from a practical point of view to characterize a power system's performance under persistent disturbances, such as load variations [17, Section D]. Yet, they are also deemed to be hard to establish, in particular in the global setting considered in the present paper [17, Section D].

The remainder of the paper is structured as follows. The SMIB model is introduced in Section 2. The stability analysis is conducted in Section 3. Section 4 presents a benchmark numerical example. The paper is concluded in Section 5 with a summary and an outlook on future work.

Notions of ISS of systems with multiple invariant sets. For the notions of ISS of systems with multiple invariant sets, we follow the conventions and definitions in [2,3,9] for dynamical systems evolving on a Riemannian manifold $\mathcal{M}$ of dimension n. Hence, the distance of a point $x \in \mathcal{M}$ from the set $S \subset \mathcal{M}$ is denoted by $|x|_S = \min_{a \in S} \Delta(x, a)$, where the symbol $\Delta(x_1, x_2)$ denotes the Riemannian distance between x_1 and x_2. Furthermore, $|x| = |x|_{\{0\}}$ denotes the usual Euclidean norm of a vector $x \in \mathbb{R}^n$. For further details on properties of dynamical systems and, in particular, systems with multiple invariant sets the reader is referred to [3,15,25] and references therein.

2. Model of a synchronous generator connected to an infinite bus

The SMIB system is introduced in this section based on [4,5,14]. We employ a generator reference direction, *i.e*, current flowing out of the SG terminals is counted positively. Following [4,5], we make some standard assumptions on the SG [14,39], which are also used in [8,23,24]: the rotor is round; the machine has one pole pair per phase; there are no damper windings and no saturation effects; there are no Eddy currents; the rotor current i_f is a real constant. The latter can be achieved by choosing the excitation voltage such that i_f is kept constant, see [8]. Furthermore, we assume that all three-phase signals are balanced [14,29]. With regards to the SG this is equivalent to assuming a "perfectly built" machine connected in star with no neutral line, see also [23,24].

We denote the three-phase voltage at the infinite bus by

$$v_{abc} := \sqrt{2}V \begin{bmatrix} \sin(\delta_g) \\ \sin(\delta_g - \frac{2\pi}{3}) \\ \sin(\delta_g + \frac{2\pi}{3}) \end{bmatrix}, \tag{2.1}$$

where $V \in \mathbb{R}_{>0}$ is the root-mean-square (RMS) value of the constant voltage amplitude (line-to-neutral) and

$$\delta_g = \delta_g(0) + \omega^s t \in \mathbb{R}, \tag{2.2}$$

with the grid frequency ω^s being a positive real constant. Furthermore, the electrical rotor angle of the SG is denoted by $\delta : \mathbb{R}_{\geq 0} \to \mathbb{R}$ and the electrical frequency by $\omega = \dot{\delta}$. As illustrated in Fig. 1, δ is the angle between the axis of coil a of the SG and the d-axis. Recall that the rotor current i_f is constant by assumption and denote the peak mutual inductance by $M_f \in \mathbb{R}_{>0}$. Then the three-phase electromotive force (EMF) $e_{abc} : \mathbb{R}_{\geq 0} \to \mathbb{R}^3$ induced in the stator is given by [14,39]

$$e_{abc} = M_f i_f \omega \begin{bmatrix} \sin(\delta) \\ \sin(\delta - \frac{2\pi}{3}) \\ \sin(\delta + \frac{2\pi}{3}) \end{bmatrix}. \tag{2.3}$$

We denote the stator resistance by $R \in \mathbb{R}_{>0}$ and the stator inductance by $L = L_s - M_s$, where $L_s \in \mathbb{R}_{>0}$ is the self-inductance and $M_s \in \mathbb{R}_{>0}$ the mutual inductance. In the SMIB scenario, the inductance and resistance of the transmission line connecting the SG to the infinite bus are often included in the parameters L and R, see [1, Section 4.13.1]. Also note that $L > 0$, since in practice $L_s > M_s$. Then the *electrical* equations describing the dynamics of the three-phase stator current $i_{abc} : \mathbb{R}_{\geq 0} \to \mathbb{R}^3$ are given by

$$L \frac{di_{abc}}{dt} = -R i_{abc} + e_{abc} - v_{abc}. \tag{2.4}$$

The SMIB model is completed with the *electromechanical* equations describing the rotor dynamics, given by

$$\begin{aligned} \dot{\delta} &= \omega, \\ J\dot{\omega} &= -D\omega + T_m - T_e, \end{aligned} \tag{2.5}$$

where the electrical torque T_e is computed as [39]

$$T_e = \omega^{-1} i_{abc}^\top e_{abc}. \tag{2.6}$$

Furthermore, $J \in \mathbb{R}_{>0}$ is the total moment of inertia of the rotor masses, $D \in \mathbb{R}_{>0}$ is the damping coefficient and $T_m \in \mathbb{R}_{\geq 0}$ is the mechanical torque provided by the prime mover, which we assume is constant.

For our stability analysis, it is convenient to perform a coordinate transformation that maps sinusoidal three-phase waveforms with constant amplitude and frequency—such as (2.1)—to constant signals. This can be achieved by representing the system (2.4), (2.5) and (2.6) in dq-coordinates via the dq-transformation given in Appendix (a). In the present case, we choose the

transformation angle

$$\varphi := \omega^s t \tag{2.7}$$

and denote the angle difference between the rotor angle δ and the dq-transformation angle φ by

$$\theta := \delta - \varphi.$$

In dq-coordinates, the grid voltage (2.1) is given by the following *constant* vector (see [29]),

$$v_{dq} = \begin{bmatrix} v_d \\ v_q \end{bmatrix} = \sqrt{3}V \begin{bmatrix} \sin(\delta_g - \varphi) \\ \cos(\delta_g - \varphi) \end{bmatrix} = \sqrt{3}V \begin{bmatrix} \sin(\delta_g(0)) \\ \cos(\delta_g(0)) \end{bmatrix},$$

where the second equality follows from (2.2). Likewise, the EMF in dq-coordinates is given by

$$e_{dq} = \begin{bmatrix} e_d \\ e_q \end{bmatrix} = \begin{bmatrix} b\omega \sin(\theta) \\ b\omega \cos(\theta) \end{bmatrix}, \tag{2.8}$$

where we have defined

$$b := \sqrt{3/2} M_f i_f. \tag{2.9}$$

Hence, the electrical torque T_e in (2.6) is given in dq-coordinates by

$$T_e = \omega^{-1} i_{abc}^\top e_{abc} = \omega^{-1} i_{dq}^\top e_{dq} = b(i_q \cos(\theta) + i_d \sin(\theta)). \tag{2.10}$$

Furthermore, with φ given in (2.7) and $T_{dq}(\cdot)$ given in (5.1), we have that

$$\frac{dT_{dq}(\varphi)}{dt} i_{abc} = \omega^s \begin{bmatrix} -i_q \\ i_d \end{bmatrix},$$

see [29, equation (4.8)]. Consequently, by replacing the rotor angle dynamics, *i.e.*, $\dot{\delta}$, with the relative rotor angle dynamics, *i.e.*, $\dot{\theta}$, the SMIB model given by (2.4), (2.5) and (2.6) becomes in dq-coordinates

$$\begin{aligned} \dot{\theta} &= \omega - \omega^s, \\ J\dot{\omega} &= -D\omega + T_m - b\left(i_q \cos(\theta) + i_d \sin(\theta)\right) + d_1(t), \\ L\dot{i}_d &= -Ri_d - L\omega^s i_q + b\omega \sin(\theta) - v_d + d_2(t), \\ L\dot{i}_q &= -Ri_q + L\omega^s i_d + b\omega \cos(\theta) - v_q + d_3(t), \end{aligned} \tag{2.11}$$

where $d(t) = \left[d_1(t), d_2(t), d_3(t)\right]^\top \in \mathbb{R}^3$ is an external perturbation which is locally essentially bounded and measurable. The signal $d(t)$ is included to capture model uncertainties originating from possible time-varying excitation current i_f, mechanical torque T_m or voltage amplitudes v_d, v_q. The model (2.11) is used for the analysis in this paper.

Remark 1. *In the related works [8,23,24] the dq-transformation angle φ is chosen as the rotor angle,* i.e., *$\varphi = \delta$. This yields $e_d = 0$ in (2.8). Furthermore, in [23,24] a dq-transformation is chosen in which the d-axis lags the q-axis by $\pi/2$. In our notation, this coordinate frame can be obtained by setting the transformation angle to $\varphi = \delta + \pi$. Hence, $e_q = b\omega$ in [8] and $e_q = -b\omega$ in [23,24]. The analysis reported in the paper can be conducted in any coordinate frame. Yet, the one employed here is independent of the rotor angle of a specific machine and, hence, seems to be more suitable to extend the results to the multi-machine case, which motivates our choice of φ.*

3. Almost global stability

This section is dedicated to the analysis of almost global stability of an equilibrium point of the system (2.11). Our analysis is conducted by employing the recently proposed framework of ISS-Leonov functions [9]. To this end, we perform the following three steps. First, we construct a suitable error system in Section 3(a). Then, we show in Section 3(b) that the set of equilibria of the

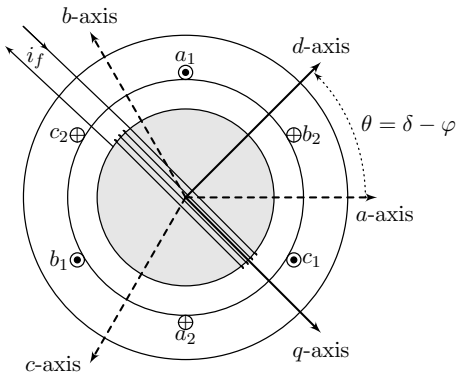

Figure 1: Schematic representation of a two-pole round-rotor SG based on [14, Figure 3.2]. The abc-axes correspond to the axes of the stator coils denoted by $a_{1,2}$, $b_{1,2}$ and $c_{1,2}$. The axis of coil a is chosen at $\theta = \delta - \varphi = 0$. The rotor current i_f flows through the rotor windings. The dq-axes denote the rotating axes of the dq-frame corresponding to the mapping $T_{dq}(\varphi)$ with φ given in (2.7) and $T_{dq}(\cdot)$ given in (5.1) of Appendix (a).

error system is decomposable in the sense of [9, Definition 3]. This is a fundamental prerequisite for the main ISS analysis—the third and final step performed in Section 3(c)—which in essence consists of verifying the conditions of [9, Theorem 3]. The almost global stability claim, given in Section 3(d), then follows in a straightforward manner from the ISS property.

For the analysis, we employ the following definition.

Definition 1. *An equilibrium point (modulo 2π) of the system (2.11) is almost globally asymptotically stable if it is asymptotically stable and for all initial conditions, except those contained in a set of zero Lebesgue measure, the solutions of the system converge to that equilibrium point (modulo 2π).*

(a) Error coordinates

It is convenient to introduce the two constants

$$c := b\sqrt{(v_d^2 + v_q^2)((L\omega^s)^2 + R^2)}, \quad \mathcal{P} := \frac{1}{c}\left[-b^2\omega^s R + (T_m - D\omega^s)((L\omega^s)^2 + R^2)\right]. \tag{3.1}$$

Note that (2.9) implies that c is nonzero if the rotor current i_f is nonzero, which is satisfied in any practical scenario.

The existence of isolated equilibria is a natural prerequisite for any stability analysis. Therefore, we make the following natural assumption that by [4, Proposition 1] implies the existence of two unique steady-state solutions (modulo 2π) of the system (2.11).

Assumption 1. *The parameters of the system (2.11) are such that $i_f > 0$ and that $|\mathcal{P}| < 1$ if $d = \underline{0}_3$ for all $t \in \mathbb{R}$.*

With Assumption 1, we denote one of the two equilibrium points of the system (2.11) by $(\theta_1^s, \omega^s, i_{d,1}^s, i_{q,1}^s)$ and introduce the error states

$$x := \left[\tilde{\theta}, \tilde{\omega}, \tilde{i}_d, \tilde{i}_q\right]^\top, \quad \theta = \tilde{\theta} + \theta_1^s,\ \omega = \tilde{\omega} + \omega^s,\ i_d = \tilde{i}_d + i_{d,1}^s,\ i_q = \tilde{i}_q + i_{q,1}^s. \tag{3.2}$$

In the error coordinates $(\tilde{\theta}, \tilde{\omega}, \tilde{i}_d, \tilde{i}_q)$ the dynamics (2.11) take the form

$$\begin{aligned}
\dot{\tilde{\theta}} =& \tilde{\omega},\\
J\dot{\tilde{\omega}} =& -D(\tilde{\omega}+\omega^s) - b(i^s_{d,1}+\tilde{i}_d)\sin(\theta^s_1+\tilde{\theta}) - b(i^s_{q,1}+\tilde{i}_q)\cos(\theta^s_1+\tilde{\theta}) + T_m + d_1(t),\\
L\dot{\tilde{i}}_d =& -R(i^s_{d,1}+\tilde{i}_d) - L\omega^s(i^s_{q,1}+\tilde{i}_q) + b(\tilde{\omega}+\omega^s)\sin(\theta^s_1+\tilde{\theta}) - v_d + d_2(t),\\
L\dot{\tilde{i}}_q =& -R(i^s_{q,1}+\tilde{i}_q) + L\omega^s(i^s_{d,1}+\tilde{i}_d) + b(\tilde{\omega}+\omega^s)\cos(\theta^s_1+\tilde{\theta}) - v_q + d_3(t).
\end{aligned} \tag{3.3}$$

Moreover, in the equilibrium point $(\theta^s_1, \omega^s, i^s_{d,1}, i^s_{q,1})$ with $d(t) = \underline{0}_3$, we have from (2.11) that

$$\begin{aligned}
0 =& -D\omega^s + T_m - b\left(i^s_{q,1}\cos(\theta^s_1) + i^s_{d,1}\sin(\theta^s_1)\right),\\
0 =& -Ri^s_{d,1} - L\omega^s i^s_{q,1} + b\omega^s\sin(\theta^s_1) - v_d,\\
0 =& -Ri^s_{q,1} + L\omega^s i^s_{d,1} + b\omega^s\cos(\theta^s_1) - v_q.
\end{aligned} \tag{3.4}$$

Hence, by using (3.4) the system (3.3) becomes in error coordinates

$$\begin{aligned}
\dot{\tilde{\theta}} =& \tilde{\omega},\\
J\dot{\tilde{\omega}} =& -D\tilde{\omega} - b\tilde{i}_d\sin(\theta^s_1+\tilde{\theta}) - bi^s_{d,1}(\sin(\theta^s_1+\tilde{\theta}) - \sin(\theta^s_1)) - b\tilde{i}_q\cos(\theta^s_1+\tilde{\theta})\\
& - bi^s_{q,1}(\cos(\theta^s_1+\tilde{\theta}) - \cos(\theta^s_1)) + d_1(t),\\
L\dot{\tilde{i}}_d =& -R\tilde{i}_d - L\omega^s\tilde{i}_q + b\omega^s(\sin(\theta^s_1+\tilde{\theta}) - \sin(\theta^s_1)) + b\tilde{\omega}\sin(\theta^s_1+\tilde{\theta}) + d_2(t),\\
L\dot{\tilde{i}}_q =& -R\tilde{i}_q + L\omega^s\tilde{i}_d + b\omega^s(\cos(\theta^s_1+\tilde{\theta}) - \cos(\theta^s_1)) + b\tilde{\omega}\cos(\theta^s_1+\tilde{\theta}) + d_3(t),
\end{aligned} \tag{3.5}$$

the equilibrium of which is now shifted to the origin. The remainder of this section is devoted to the analysis of this system.

Remark 2. *As can be seen from* (2.9)*, the signs of* c *and, hence,* $\mathcal{P}$ *defined in* (3.1) *depend on the sign of the constant rotor current* i_f*. For the subsequent analysis, it is important to know the sign of* c*, as it determines which of the two equilibria of the system* (2.11) *is stable. Assumption* 1 *is made without loss of generality because the analysis for* $i_f < 0$ *follows* verbatim.

(b) Decomposable invariant set containing all equilibria

With Assumption 1, the system (3.5) has a finite and disjoint set of equilibria (modulo 2π) in the sense of [9, Definition 3]. Denote this set by

$$\mathcal{W} = \left\{\underline{0}_4 \cup \left([\theta^s_2, \omega^s, i^s_{d,2}, i^s_{q,2}]^\top - [\theta^s_1, \omega^s, i^s_{d,1}, i^s_{q,1}]^\top\right)\right\}. \tag{3.6}$$

The lemma below shows that—for bounded solutions—$\mathcal{W}$ contains all α- and ω-limit sets of the system (3.5)—see [2,3,9] for details. This feature is instrumental to apply the ISS-Leonov framework [9] and establish our main result.

Lemma 1. *Consider the system* (3.5) *with Assumption* 1*. Suppose that all its solutions are bounded and that*

$$4RD[(L\omega^s)^2 + R^2] > (Lb\omega^s)^2. \tag{3.7}$$

Then the set $\mathcal{W}$ *is decomposable in the sense of [9, Definition 3] and contains all* α*- and* ω*-limit sets of the system* (3.5)*.*

Proof. In order to show that the set $\mathcal{W}$ contains all α-and ω-limit sets of (3.5) and that it is decomposable, note that the electrical dynamics in (3.5) takes the form

$$L\dot{\tilde{i}}_{dq} = \begin{bmatrix} u \\ w \end{bmatrix} + \begin{bmatrix} b\tilde{\omega}\sin(\theta_1^s + \tilde{\theta}) \\ b\tilde{\omega}\cos(\theta_1^s + \tilde{\theta}) \end{bmatrix}, \tag{3.8}$$

where we defined

$$\begin{bmatrix} u \\ w \end{bmatrix} := \begin{bmatrix} -R & -L\omega^s \\ L\omega^s & -R \end{bmatrix} \tilde{i}_{dq} + \begin{bmatrix} b\omega^s(\sin(\tilde{\theta} + \theta_1^s) - \sin(\theta_1^s)) \\ b\omega^s(\cos(\tilde{\theta} + \theta_1^s) - \cos(\theta_1^s)) \end{bmatrix}.$$

Following [4], consider the function

$$W(x) = \frac{L}{2}(u^2 + w^2) + \frac{J\tilde{\omega}^2}{2}\left[(L\omega^s)^2 + R^2\right] + q(\tilde{\theta}), \tag{3.9}$$

where x is defined in (3.2),

$$q(\tilde{\theta}) = c[-\cos(\theta_1^s - \phi + \tilde{\theta}) - \sin(\theta_1^s - \phi)\tilde{\theta} + \cos(\theta_1^s - \phi)] \tag{3.10}$$

and[1]

$$\phi = \arctan\left(\frac{L\omega^s v_d + Rv_q}{L\omega^s v_q - Rv_d}\right). \tag{3.11}$$

Clearly, W is continuously differentiable as a function $W : \mathbb{R}^4 \to \mathbb{R}$ (but not as a function $W : \mathbb{S} \times \mathbb{R}^3 \to \mathbb{R}$, where $\mathbb{S}$ denotes the unit circle). With (3.5), a lengthy but straightforward calculation yields

$$\begin{aligned} \dot{W} =& -R[u^2 + w^2] - D((L\omega^s)^2 + R^2)\tilde{\omega}^2 + \tilde{\omega}u\, Lb\omega^s\cos(\tilde{\theta} + \theta_1^s) - \tilde{\omega}w\, Lb\omega^s\sin(\tilde{\theta} + \theta_1^s) \\ &+ d_1\tilde{\omega}((L\omega^s)^2 + R^2) + d_2(L\omega^s w - Ru) - d_3(L\omega^s u + Rw), \\ =& -\begin{bmatrix} \tilde{\omega} & u & w \end{bmatrix} M \begin{bmatrix} \tilde{\omega} & u & w \end{bmatrix}^\top - \begin{bmatrix} \tilde{\omega} & u & w \end{bmatrix} M_d d, \end{aligned}$$

where

$$M = \begin{bmatrix} D((L\omega^s)^2 + R^2) & -\frac{Lb\omega^s\cos(\tilde{\theta}+\theta_1^s)}{2} & \frac{Lb\omega^s\sin(\tilde{\theta}+\theta_1^s)}{2} \\ -\frac{Lb\omega^s\cos(\tilde{\theta}+\theta_1^s)}{2} & R & 0 \\ \frac{Lb\omega^s\sin(\tilde{\theta}+\theta_1^s)}{2} & 0 & R \end{bmatrix}, \; M_d = \begin{bmatrix} -\left((L\omega^s)^2 + R^2\right) & 0 & 0 \\ 0 & R & L\omega^s \\ 0 & -L\omega^s & R \end{bmatrix}. \tag{3.12}$$

In order to show that $\mathcal{W}$ indeed contains all α- and ω-limit sets of (3.5), we consider the nominal version of the system (3.5), *i.e.*, with $d(t) = \underline{0}_3$ for all $t \in \mathbb{R}$. Since $R > 0$, the Schur-complement implies that $M > 0$ if and only if (3.7) holds. Then, we have immediately that (3.7) implies that

$$\dot{W} \leq 0.$$

Consequently, by invoking LaSalle's invariance principle [31] we conclude that all bounded solutions of the nominal system (3.5) converge to the set where

$$\tilde{\omega} = w = u = 0 \quad \forall t \in \mathbb{R}. \tag{3.13}$$

From (3.8) we have that $\tilde{\omega} = w = u = 0$ implies $\tilde{i}_{dq}$ constant. Since $\tilde{\omega} = 0$ also implies $\tilde{\theta}$ constant, $\mathcal{W}$ is the only invariant set under the restriction (3.13) and it contains all α- and ω-limit sets of (3.5). Consequently, if $d(t) = \underline{0}_3$ for all $t \in \mathbb{R}$, then $\dot{W} \leq 0$ implies that $\mathcal{W}$ is decomposable in the sense of [9, Definition 3], completing the proof. □

[1]Here $\arctan(\cdot)$ denotes the standard arctangent function defined on the interval $[0, \pi)$. Since the case $v_d = v_q = 0$ is excluded by definition of v_d and v_q, ϕ is well-defined.

(c) A condition for ISS

Recall the function $q(\tilde{\theta})$ defined in (3.10) and let

$$h(\tilde{\theta}) = q(\tilde{\theta}) - \frac{\epsilon}{2}\tilde{\theta}^2, \tag{3.14}$$

where ϵ is a positive real parameter. Denote

$$\epsilon_{\min} := \inf\left\{\epsilon \in \mathbb{R}_{>0} \mid h(\tilde{\theta}) \leq 0 \quad \forall \tilde{\theta} \in \mathbb{R}\right\}. \tag{3.15}$$

It is shown in [4, Lemma 1] that $c > 0$ defined in (3.1) is an upper bound for $\epsilon_{\min}$, *i.e.*, the infimum in (3.15) is indeed always achievable. The lemma below is useful to establish our main ISS result.

Lemma 2. *Let $\epsilon > \epsilon_{\min}$. Then for all $\tilde{\theta} \in \mathbb{R}$ and any $\varepsilon \in [0, \epsilon - \epsilon_{\min})$,*

$$-\frac{\epsilon}{2}\tilde{\theta}^2 \leq h(\tilde{\theta}) \leq -\frac{\varepsilon}{2}\tilde{\theta}^2.$$

Proof. By the definition of $\epsilon_{\min}$ we have that

$$\bar{h}(\tilde{\theta}) := q(\tilde{\theta}) - \frac{\epsilon_{\min}}{2}\tilde{\theta}^2 \leq 0.$$

Hence,

$$h(\tilde{\theta}) = \bar{h}(\tilde{\theta}) - \frac{1}{2}(\epsilon - \epsilon_{\min})\tilde{\theta}^2 \leq -\frac{1}{2}(\epsilon - \epsilon_{\min})\tilde{\theta}^2 \leq -\frac{\varepsilon}{2}\tilde{\theta}^2$$

for any $\varepsilon \in [0, \epsilon - \epsilon_{\min})$. To derive the lower bound for h, we note that since $\epsilon > \epsilon_{\min}$,

$$-\frac{\epsilon}{2}\tilde{\theta}^2 \leq h(\tilde{\theta}) \Leftrightarrow 0 \leq h(\tilde{\theta}) + \frac{\epsilon}{2}\tilde{\theta}^2 = \bar{h}(\tilde{\theta}) - \frac{1}{2}(\epsilon - \epsilon_{\min})\tilde{\theta}^2 + \frac{\epsilon}{2}\tilde{\theta}^2 \leq -\frac{1}{2}(\epsilon - \epsilon_{\min})\tilde{\theta}^2 + \frac{\epsilon}{2}\tilde{\theta}^2 \leq \frac{\epsilon}{2}\tilde{\theta}^2,$$

completing the proof. □

To streamline the presentation of our result the following assumption is needed. A physical interpretation of this key assumption is given in the discussion in Remark 4 below.

Assumption 2. *There exist constants $\chi > 0$ and $\psi > 0$ satisfying*

$$\bar{\mathcal{Q}} = \begin{bmatrix} \frac{\chi}{2\epsilon_{\min}} & 1 & 0 \\ 1 & \left((L\omega^s)^2 + R^2\right)\left(D - \frac{\chi J}{2} - \frac{\psi}{4}\right) & Lb\omega^s \\ 0 & Lb\omega^s & 4\left(R - \frac{\chi L}{2}\right) - \psi \end{bmatrix} > 0. \tag{3.16}$$

In addition, we borrow the following result from [4].

Lemma 3. *[4] Consider the system (3.5) verifying Assumptions 1 and 2. Then, all solutions $x = \left[\tilde{\theta}, \tilde{\omega}, \tilde{i}_d, \tilde{i}_q\right]^\top$ of the system (3.5) are bounded.*

We are now in a position to present our ISS result.

Theorem 1. *Consider the system (3.5) with Assumptions 1 and 2. The system (3.5) is ISS with respect to the set $\mathcal{W}$ defined in (3.6).*

Proof. Note that Lemma 3 implies that all solutions of the system (3.5) are bounded under Assumption 2. Moreover, we see that $\bar{\mathcal{Q}} > 0$ in (3.16) reduces to (3.7) for $\chi = \psi = 0$. As $\bar{\mathcal{Q}} > 0$ for some $\chi > 0$, $\psi > 0$ by assumption, the condition of Lemma 1 is met. Consequently, the set $\mathcal{W}$ is decomposable and contains all α- and ω-limit sets of the system (3.5).

The remainder of the claim is established by invoking [9, Theorem 3]. To this end, we need to construct a function V, that—along all solutions of the system (3.5)—satisfies the following two properties

$$\alpha_1(|x|_{\mathcal{W}}) - \sigma(|\tilde{\theta}|) \leq V(x) \leq \alpha_2(|x|_{\mathcal{W}} + g) \tag{3.17}$$

and

$$\dot{V}(x) \leq -\lambda(V(x)) + \gamma(|d|), \tag{3.18}$$

where $g \geq 0$ is a scalar, $\alpha_1 \in \mathcal{K}_\infty$, $\alpha_2 \in \mathcal{K}_\infty$, $\sigma \in \mathcal{K}_\infty$, $\gamma \in \mathcal{K}_\infty$, and $\lambda : \mathbb{R} \to \mathbb{R}$ is a continuous function satisfying $\lambda \in \mathcal{K}_\infty$ for nonnegative arguments. Following [9, Definition 7], such function V is called an ISS-Leonov function[2].

Recall W defined in (3.9), h defined in (3.14) and consider the following ISS-Leonov function candidate $V : \mathbb{R}^4 \to \mathbb{R}$,

$$V(x) = \frac{L}{2}(u^2 + w^2) + \frac{J\tilde{\omega}^2}{2}\left[(L\omega^s)^2 + R^2\right] + h(\tilde{\theta}). \tag{3.19}$$

In the first step of the proof, we show that V satisfies condition (3.17). Note that Lemma 2 implies that for all $x \in \mathbb{R}^4$,

$$\begin{aligned}\frac{L}{2}(u^2 + w^2) + \frac{J\tilde{\omega}^2}{2}\left[(L\omega^s)^2 + R^2\right] - \frac{\epsilon}{2}|\tilde{\theta}|^2 \leq V(x) \leq \frac{L}{2}(u^2 + w^2) + \frac{J\tilde{\omega}^2}{2}\left[(L\omega^s)^2 + R^2\right] - \frac{\varepsilon}{2}|\tilde{\theta}|^2 \\ \leq \kappa|(\tilde{\theta}, \tilde{\omega}, \tilde{i}_d, \tilde{i}_q)|_{\mathcal{W}}\end{aligned}$$

for some real $\kappa > 0$. Thus, property (3.17) is satisfied.

The second and last step of the proof consists in verifying condition (3.18). Recall M and M_d given in (3.12). Differentiating V given in (3.19) along solutions of the system (3.5) yields

$$\begin{aligned}\dot{V} &= -\begin{bmatrix}\tilde{\omega}\\ u\\ w\end{bmatrix}^\top M \begin{bmatrix}\tilde{\omega}\\ u\\ w\end{bmatrix} - \begin{bmatrix}\tilde{\omega}\\ u\\ w\end{bmatrix}^\top M_d d - \epsilon\tilde{\theta}\tilde{\omega} \\ &= -\begin{bmatrix}x\\ d\end{bmatrix}^\top \underbrace{\begin{bmatrix}\mathcal{Q}_x & \mathcal{Q}_{xd}\\ \mathcal{Q}_{xd}^\top & \gamma I_3\end{bmatrix}}_{:=\mathcal{Q}} \begin{bmatrix}x\\ d\end{bmatrix} - \chi\left(\frac{L}{2}(u^2 + w^2) + \frac{J\tilde{\omega}^2}{2}\left[(L\omega^s)^2 + R^2\right] - \frac{\varepsilon}{2}|\tilde{\theta}|^2\right) + \gamma|d|^2,\end{aligned} \tag{3.20}$$

where

$$\mathcal{Q}_x = \begin{bmatrix}\frac{1}{2}\chi\varepsilon & \frac{1}{2}\epsilon & 0 & 0\\ \frac{1}{2}\epsilon & ((L\omega^s)^2 + R^2)(D - \frac{\chi J}{2}) & -\frac{Lb\omega^s\cos(\tilde{\theta}+\theta_1^s)}{2} & \frac{Lb\omega^s\sin(\tilde{\theta}+\theta_1^s)}{2}\\ 0 & -\frac{Lb\omega^s\cos(\tilde{\theta}+\theta_1^s)}{2} & R - \frac{\chi L}{2} & 0\\ 0 & \frac{Lb\omega^s\sin(\tilde{\theta}+\theta_1^s)}{2} & 0 & R - \frac{\chi L}{2}\end{bmatrix}, \quad \mathcal{Q}_{xd} = \begin{bmatrix}0_{1\times 3}\\ \frac{1}{2}M_d\end{bmatrix}.$$

We need to verify that $\mathcal{Q} \geq 0$. Since $\gamma > 0$, the Schur complement implies that $\mathcal{Q} \geq 0$ if and only if

$$\mathcal{Q}_x - \frac{1}{\gamma}\mathcal{Q}_{xd}\mathcal{Q}_{xd}^\top = \mathcal{Q}_x - \frac{1}{4\gamma}\begin{bmatrix}0 & 0 & 0 & 0\\ 0 & ((L\omega^s)^2 + R^2)^2 & 0 & 0\\ 0 & 0 & (L\omega^s)^2 + R^2 & 0\\ 0 & 0 & 0 & (L\omega^s)^2 + R^2\end{bmatrix} \geq 0. \tag{3.21}$$

[2]From (3.17), we see that the sign definiteness requirements of an ISS-Leonov function are relaxed compared to the standard Lyapunov function, because V does not have to be positive definite with respect to the variable $\tilde{\theta}$, *i.e.,* the variable with respect to which the dynamics (3.5) is periodic. Furthermore, the time-derivative of V only needs to be negative definite for positive values of V. See [9] for further details.

Furthermore, since $\chi > 0$, $\varepsilon > 0$ and $\gamma > 0$, applying the Schur complement also to the matrix in (3.21) implies that $\mathcal{Q} \geq 0$ if and only if

$$R - \frac{\chi L}{2} - \frac{1}{4\gamma}\left((L\omega^s)^2 + R^2\right) > 0 \tag{3.22}$$

and

$$((L\omega^s)^2 + R^2)\left(D - \frac{\chi J}{2}\right) - \frac{1}{4\gamma}((L\omega^s)^2 + R^2)^2 - \frac{\epsilon^2}{2\chi\varepsilon} - \frac{(Lb\omega^s)^2}{4(R - \chi\frac{L}{2} - \frac{1}{4\gamma}((L\omega^s)^2 + R^2))} \geq 0. \tag{3.23}$$

Recall from Lemma 2 that $0 < \varepsilon < \epsilon - \epsilon_{\min}$. Hence, the left-hand side of (3.23) attains its maximum with respect to ε for $\varepsilon = \epsilon - \epsilon_{\min}$. We select this value for ε and proceed by requiring (3.23) to be satisfied with strict inequality. This ensures that there exists a $0 < \varepsilon < \epsilon - \epsilon_{\min}$ for which $\mathcal{Q} \geq 0$. It is then straightforward to verify that this implies that the expression on the left-hand side of (3.23) attains its maximum with respect to ϵ for $\epsilon = 2\epsilon_{\min} > \epsilon_{\min}$. For this choice of ϵ (3.23) becomes

$$((L\omega^s)^2 + R^2)\left(D - \frac{\chi J}{2}\right) - \frac{1}{4\gamma}((L\omega^s)^2 + R^2)^2 - \frac{2\epsilon_{\min}}{\chi} - \frac{(Lb\omega^s)^2}{4(R - \frac{\chi L}{2}) - \frac{1}{\gamma}((L\omega^s)^2 + R^2)} > 0. \tag{3.24}$$

Hence, by defining the auxiliary variable $\psi = ((L\omega^s)^2 + R^2)\gamma^{-1} > 0$, (3.23) being satisfied with strict inequality is equivalent to positive definiteness of the matrix $\bar{\mathcal{Q}}$ in (3.16). Clearly, $\bar{\mathcal{Q}} > 0$ also implies that (3.22) is satisfied. Recall that $\bar{\mathcal{Q}} > 0$ by Assumption 2. Hence, $\mathcal{Q} \geq$ and

$$\dot{V} \leq -\chi V + \gamma|d|^2, \tag{3.25}$$

which is property (3.18). Consequently, with Assumption 2, V satisfies conditions (3.17) and (3.18), which implies that V is an ISS-Leonov function for the system (3.5). Hence, by invoking [9, Theorem 3] (or, equivalently, [9, Corollary 1]) it follows that the system (3.5) is ISS with respect to the set $\mathcal{W}$. This completes the proof. □

Remark 3. *The ISS-Leonov function V defined in (3.19) is not periodic in $\tilde{\theta}$. Thus, it does not qualify as a usual ISS Lyapunov function [3]. Yet, this non-periodicity of V in $\tilde{\theta}$ is essential for being able to treat the constant terms in the dynamics (3.5) and to establish the ISS claim in Proposition 1. Furthermore, in order to ensure continuity of the ISS-Leonov function in (3.19) it is necessary to consider the angle $\tilde{\theta}$ evolving in $\mathbb{R}$ rather than, as usual, on the torus $\mathbb{S}$. The same applies to the function W defined in (3.9). In $\mathbb{R}$, $\tilde{\theta}$ is not bounded* a priori. *While it is shown in [9, Theorem 3] that existence of an ISS-Leonov function with $\tilde{\theta} \in \mathbb{R}$ ensures boundedness of the distance $|x|_{\mathcal{W}}$ with $x \in \mathbb{S} \times \mathbb{R}^3$, this does not imply boundedness of $|x|_{\mathcal{W}}$ for $x \in \mathbb{R}^4$. Since boundedness of solutions is a fundamental prerequisite to invoke Lemma 1 (that ensures decomposability of $\mathcal{W}$), we need the auxiliary Lemma 3 to establish boundedness of solutions of the system (3.5) evolving in $\mathbb{R}^4$.*

Remark 4. *By using the standard definitions for the reactance X, the conductance G and the susceptance B [1,16],* i.e.,

$$X = \omega^s L, \quad G = \frac{R}{R^2 + X^2}, \quad B = -\frac{X}{R^2 + X^2},$$

condition (3.7)—which is implied by Assumption 2—can be rewritten as

$$4DG(R^2 + X^2)^2 > X^2 b^2 \quad \Leftrightarrow \quad 4D\frac{R}{X} > |B|b^2.$$

This shows that a high damping factor D and a high R/X ratio, i.e., *a high electrical dissipation, are beneficial to ensure ISS of the system (3.5) with respect to the equilibrium set $\mathcal{W}$. On the contrary, a high value of $|b|$,* i.e., *a high excitation and consequently large EMF amplitude, deteriorate the likelihood of verifying the ISS property for the system (3.5). Both observations are sensible from a physical perspective and consistent with practical experience.*

(d) Main stability result

We give now conditions for almost global asymptotic stability of one of the two equilibria (modulo 2π) of the system (2.11). This result follows as a corollary of Theorem 1 after the relaxation of Assumption 2—setting $\psi = 0$—as indicated below.

Corollary 1. *Consider the system* (3.5) *with Assumption* 1. *Suppose that* $d(t) = \underline{0}_3$ *for all* $t \in \mathbb{R}$ *and that Assumption* 2 *is satisfied for* $\psi = 0$. *Then, the equilibrium point* $(\theta_1^s, \omega^s, i_d^s, i_q^s)$ *satisfying* $|\theta_1^s - \phi| < \frac{\pi}{2}$ *(modulo* 2π*) with* ϕ *defined in* (3.11) *is almost globally asymptotically stable,* i.e., *for all initial conditions, except a set of measure zero, the solutions of the system* (2.11) *asymptotically converge to that equilibrium point.*

Proof. For $d(t) = \underline{0}_3$ for all $t \in \mathbb{R}$, we have that $\gamma = 0$ in $\mathcal{Q}$ in (3.20). Hence, $\mathcal{Q} \geq 0$ is equivalent to $\mathcal{Q}_x \geq 0$, see (3.20). By following the proof of Theorem 1, with $\epsilon = 2\epsilon_{\min}$, we see that $\mathcal{Q}_x \geq 0$ is implied by $\bar{\mathcal{Q}} > 0$ for $\psi = 0$. As the latter holds by assumption, it follows that, see (3.25),

$$\dot{V} \leq -\chi V. \tag{3.26}$$

This shows that for all initial conditions, the solutions of the system (3.5) asymptotically converge to the set $\mathcal{W}$. Recall from the proof of Theorem 1 that, under the standing assumptions, $\dot{W} \leq 0$. Furthermore, by the definition of $q(\tilde{\theta})$ in (3.10), we have that

$$q(0) = 0, \quad q'(0) = 0, \quad q''(0) = c\cos(\theta_1^s - \phi).$$

Hence, the function W defined in (3.9) has a local minimum at the origin if $|\theta_1^s - \phi| < \frac{\pi}{2}$, while it has a local maximum at $|\theta_1^s - \phi| > \frac{\pi}{2}$. Therefore, if $|\theta_1^s - \phi| < \frac{\pi}{2}$, the origin is locally asymptotically stable, while it is unstable if $|\theta_1^s - \phi| > \frac{\pi}{2}$.

To establish almost global asymptotic stability of the equilibrium point satisfying $|\theta_1^s - \phi| < \frac{\pi}{2}$, we follow [5] and invoke [22, Proposition 11]. To this end, consider the Jacobian of the system (3.5) evaluated at an equilibrium point, *i.e.*,

$$\mathcal{J} = \begin{bmatrix} 0 & 1 & 0 & 0 \\ \frac{b}{J}\left(i_q^s \sin(\theta^s) - i_d^s \cos(\theta^s)\right) & -\frac{D}{J} & -\frac{b}{J}\sin(\theta^s) & -\frac{D}{J}\cos(\theta^s) \\ \frac{b}{L}\omega^s \cos(\theta^s) & \frac{b}{L}\sin(\theta^s) & -\frac{R}{L} & -\omega^s \\ -\frac{b}{L}\omega^s \sin(\theta^s) & \frac{b}{L}\cos(\theta^s) & \omega^s & -\frac{R}{L} \end{bmatrix}.$$

By using (3.4) and (3.11), we obtain

$$\det(\mathcal{J}) = \frac{b\cos(\theta^s - \phi)}{J\sqrt{R^2 + (L\omega^s)^2}}.$$

Hence, $\det(\mathcal{J}) < 0$ if $|\theta^s - \phi| > \frac{\pi}{2}$, *i.e.*, if the considered equilibrium point is unstable. Furthermore, $\mathcal{J}$ is a real-valued matrix of dimension 4. Consequently, if $\det(\mathcal{J}) < 0$, then $\mathcal{J}$ has at least one positive real eigenvalue and from [22, Proposition 11] it follows that the region of attraction of the unstable equilibrium has zero Lebesgue measure. Hence, for all initial conditions, except a set of measure zero, the solutions of the system (3.5) asymptotically converge to the equilibrium point $(\theta_1^s, \omega^s, i_d^s, i_q^s)$ satisfying $|\theta_1^s - \phi| < \frac{\pi}{2}$ (modulo 2π). This completes the proof. □

4. Numerical example

The analysis is illustrated on a numerical benchmark example with data taken from [1, Table D.2, H16]. All system parameters are given in per unit (pu) including normalized time (for $\omega_{\text{Base}} = 2\pi 60\text{rad/sec}$), see Table 1. Furthermore, based on [1, Example 5.1], we assume a line resistance of

Table 1: Parameters of the system (3.5) taken from [1, Table D.2, H16]

Parameter	Numerical value in pu	Parameter	Numerical value in pu
ω^s	1	J	$3 \cdot 2558.9$
D_{nom}	$3 \cdot 2$	V	1
R	0.0221	L	1.21

$R_\ell = 0.02$ pu and a line inductance of $L_\ell = 0.4$ pu. The nominal damping coefficient is given by $D_{\text{nom}} = 3 \cdot 2$ pu (see [1, Table D.2])[3].

Condition (3.16) is a linear matrix inequality (LMI) with decision variables $\chi > 0$ and $\psi > 0$. Hence, its feasibility can be verified efficiently using standard software tools, such as Yalmip [20]. For the subsequent experiments we take D as additional decision variable and seek to determine the minimal damping coefficient $D_{\min}$ required for our condition (3.16) to be satisfied. Thereby, following our previous work [4,5], we consider a large variety of operating scenarios. More precisely, we modify the machine loading by varying T_m, as well as the excitation by varying i_f. All other parameters are kept constant. Furthermore, we define the error coordinates x in (3.2) with respect to the unstable equilibrium point, *i.e.*, satisfying $|\theta_1^s - \phi| > \frac{\pi}{2}$.

The resulting values for $D_{\min}$ are shown in Figure 2a. Since the machine torque T_e is normalized with respect to the single-phase power base, the rated torque corresponds to $T_e^s = 3.0$ pu. Also, usually it is only possible to load large SGs at their rated power if the amplitude of the EMF e_{abc} is higher than the rated voltage [30, Chapter 5]. This explains the chosen ranges of values for E^s and T_e^s in Figure 2a. By Theorem 1 the SMIB system (3.5) is ISS with respect to the corresponding equilibrium set $\mathcal{W}$ (if it exists) for any damping coefficient $D \geq D_{\min}$. Furthermore, by Corollary 1 we conclude that—for $d(t) = \underline{0}_3$ for all $t \geq 0$—the equilibrium point with $|\theta_1^s - \phi| < \frac{\pi}{2}$ (modulo 2π) with ϕ defined in (3.11) is almost globally asymptotically stable. Both properties are further illustrated in Figure 2b for $D = 62.4 D_{\text{nom}}$, $T_e^s = 3$pu and $|E^s| = 1.566$pu. The bold lines correspond to the case $d(t) = \underline{0}_3$, while the dashed lines correspond to the case $d_1 = 0.25\sin(3t)$, $d_2 = 0.5\sin(5t)$, $d_3 = 0.3\sin(t)$. It can be seen from the simulation results that the trajectories of the perturbed system (*i.e.*, $d(t) \neq \underline{0}_3$) remain close to those of the unperturbed system (*i.e.*, $d(t) = \underline{0}_3$), as predicted by the ISS property.

Moreover, in line with the observations made in [4,5], Figure 2a shows that the required damping increases with the machine loading and the excitation magnitude. This is consistent with the well-known power-angle characteristic that can be employed for reduced-order SG models and states that the likelihood of an SG to undergo instability after a change in load increases with the SG being operated closer to its generation limit [14,21].

5. Conclusions

A global stability analysis of the equilibria of a realistic SMIB model has been presented. The main result is established by using the powerful property of ISS, which is verified using an ISS-Leonov function for periodic systems with multiple invariant sets—an approach first advocated in [9]. Compared to the usual Lyapunov functions, ISS-Leonov functions have the advantage that the the conditions of sign definiteness imposed are obviated. This key feature turns out to be

[3]The scaling factor 3 in J and D originates from the following fact. In [1], the mechanical equation (2.5) is expressed in pu with respect to the 3-phase base power $S_{3\phi}$. Hence, the pu values of J, D, T_m and T_e are also expressed with respect to $S_{3\phi}$. In the model (2.5), the electrical torque T_e in (2.10) is expressed with respect to the single-phase power $\frac{S_{3\phi}}{3}$. Consequently, one way to match our model (2.5) with the parameters in [1] is to scale J and D by a factor 3, *i.e.*, to represent the mechanical equation (2.5) with respect to the power base $\frac{S_{3\phi}}{3}$.

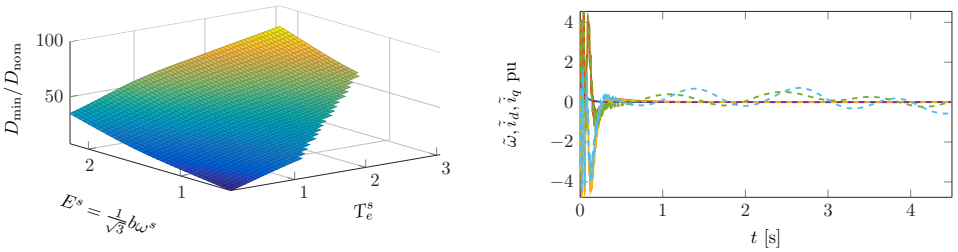

(a) Minimum required damping coefficient $D_{\min}$ compared to nominal damping coefficient D_{nom} for condition (3.16) to be satisfied in a broad range of operating conditions.

(b) Simulation results for the system (3.5). The solid lines show the state trajectories of $\tilde{\omega}, \tilde{i}_d, \tilde{i}_q$ for the case $d(t) = \underline{0}_3$. The dashed lines correspond to the case $d_1 = 0.25\sin(3t)$, $d_2 = 0.5\sin(5t)$, $d_3 = 0.3\sin(t)$.

Figure 2: Numerical evaluation of the conditions (3.16) and illustration of the ISS property.

essential for the analysis of the SMIB system carried out in this paper. The conservativeness of the derived conditions has been assessed via extensive numerical evaluations on a benchmark problem.

Our current research is directed towards the development of transient stability analysis methods for power system models with time-dependent transmission lines and physically more realistic SG models (*e.g.*, considering torque and voltage control loops as well as saturation effects), which is a natural extension of the presented results. Given the "scalable" nature of the analysis tools employed here this seems a feasible—albeit difficult—task. Another objective is to further reduce the conservativeness of the conditions by improving the construction of the employed Lyapunov function.

Appendix

(a) The dq-transformation

The dq-transformation employed in the model derivation of the SMIB model in Section 2 is stated, see [1,21,29]. Let $x : \mathbb{R}_{\geq 0} \to \mathbb{R}^3$ be a balanced three-phase signal, cf. (2.3), (2.1), and $\varrho : \mathbb{R}_{\geq 0} \to \mathbb{R}$. Consider the mapping $T_{dq} : \mathbb{R} \to \mathbb{R}^{2\times 3}$,

$$T_{dq}(\varrho) := \sqrt{\frac{2}{3}} \begin{bmatrix} \cos(\varrho) & \cos(\varrho - \frac{2}{3}\pi) & \cos(\varrho + \frac{2}{3}\pi) \\ \sin(\varrho) & \sin(\varrho - \frac{2}{3}\pi) & \sin(\varrho + \frac{2}{3}\pi) \end{bmatrix}. \tag{5.1}$$

Then, $f_{dq} : \mathbb{R}^3 \times \mathbb{R} \to \mathbb{R}^2$,

$$f_{dq}(x(t), \varrho(t)) = T_{dq}(\varrho(t))x(t)$$

is called dq-transformation.

Authors' Contributions. The research design, theoretical results and numerics were performed by J.S. and supported by D.E. with R.O. and N.B. supervising the work. All authors contributed to editing the manuscript.

Competing Interests. The author(s) declare that they have no competing interests.

Funding. This work was partially supported by the Government of Russian Federation (Grant 074-U01) and the Ministry of Education and Science of Russian Federation (Project 14.Z50.31.0031).

References

1. P. Anderson and A. Fouad, *Power System Control and Stability*. J.Wiley & Sons, 2002.
2. D. Angeli and D. Efimov, "On input-to-state stability with respect to decomposable invariant sets," in *52nd IEEE Conference on Decision and Control*. IEEE, 2013, pp. 5897–5902.

3. ——, "Characterizations of input-to-state stability for systems with multiple invariant sets," *IEEE Transactions on Automatic Control*, vol. 60, no. 12, pp. 3242–3256, 2015.
4. N. Barabanov, J. Schiffer, R. Ortega, and D. Efimov, "Almost global attractivity of a synchronous generator connected to an infinite bus," in *55th Conference on Decision and Control*, 2016, pp. 4130–4135.
5. ——, "Conditions for almost global attractivity of a synchronous generator connected to an infinite bus," *IEEE Transactions on Automatic Control*, 2016, submitted.
6. H.-P. Beck and R. Hesse, "Virtual synchronous machine," in *9th Int. Conf. on Electr. Power Quality and Utilisation.*, Oct. 2007, pp. 1–6.
7. S. Y. Caliskan and P. Tabuada, "Uses and abuses of the swing equation model," in *54th IEEE Conference on Decision and Control*, 2015, pp. 6662–6667.
8. S. Caliskan and P. Tabuada, "Compositional transient stability analysis of multimachine power networks," *IEEE Transactions on Control of Network Systems*, vol. 1, no. 1, pp. 4–14, March 2014.
9. D. Efimov, J. Schiffer, N. Barabanov, and R. Ortega, "A relaxed characterization of ISS for periodic systems with multiple invariant sets," 2016, submitted.
10. D. Efimov, J. Schiffer, and R. Ortega, "Robustness of delayed multistable systems with application to droop-controlled inverter-based microgrids," *International Journal of Control*, vol. 89, no. 5, pp. 909–918, 2016.
11. H. Farhangi, "The path of the smart grid," *IEEE Power and Energy Magazine*, vol. 8, no. 1, pp. 18–28, Jan. 2010.
12. S. Fiaz, D. Zonetti, R. Ortega, J. Scherpen, and A. van der Schaft, "A port-hamiltonian approach to power network modeling and analysis," *European Journal of Control*, vol. 19, no. 6, pp. 477–485, 2013.
13. A. K. Gelig, G. Leonov, and V. Yakubovich, "Stability of nonlinear systems with nonunique equilibrium position," *Moscow Izdatel Nauka*, vol. 1, 1978.
14. J. J. Grainger and W. D. Stevenson, *Power System Analysis*. McGraw-Hill New York, 1994, vol. 621.
15. J. Guckenheimer and P. Holmes, *Nonlinear Oscillations, Dynamical Systems, and Bifurcations of Vector Fields*, ser. Applied Mathematical Sciences. New York: Springer-Verlag, 1983, vol. 42.
16. P. Kundur, *Power System Stability and Control*. McGraw-Hill, 1994.
17. P. Kundur, J. Paserba, V. Ajjarapu, G. Andersson, A. Bose, C. Canizares, N. Hatziargyriou, D. Hill, A. Stankovic, C. Taylor, T. Van Cutsem, and V. Vittal, "Definition and classification of power system stability IEEE/CIGRE joint task force on stability terms and definitions," *IEEE Transactions on Power Systems*, vol. 19, no. 3, pp. 1387–1401, 2004.
18. G. Leonov, "Phase synchronisation. theory and applications," *Nonlinear Systems: Frequency and Matrix Inequalities*, 2008.
19. ——, "On the boundedness of the trajectories of phase systems," *Siberian Mathematical Journal*, vol. 15, no. 3, pp. 491–495, 1974.
20. J. Löfberg, "YALMIP : a toolbox for modeling and optimization in MATLAB," in *IEEE International Symposium on Computer Aided Control Systems Design*, sept. 2004, pp. 284 –289.
21. J. Machowski, J. Bialek, and J. Bumby, *Power System Dynamics: Stability and Control*. J.Wiley & Sons, 2008.
22. P. Monzón and R. Potrie, "Local and global aspects of almost global stability," in *45th IEEE Conf. on Decision and Control*, Dec. 2006, pp. 5120–5125.
23. V. Natarajan and G. Weiss, "Almost global asymptotic stability of a constant field current synchronous machine connected to an infinite bus," in *Proc. of the 53rd IEEE Conference on Decision and Control*, 2014, pp. 3272–3279.
24. ——, "A method for proving the global stability of a synchronous generator connected to an infinite bus," in *2014 IEEE 28th Convention of Electrical & Electronics Engineers in Israel (IEEEI)*. IEEE, 2014, pp. 1–5.
25. Z. Nitecki and M. Shub, "Filtrations, decompositions, and explosions," *American Journal of Mathematics*, vol. 97, no. 4, pp. 1029–1047, 1975.
26. E. J. Noldus, "New direct Lyapunov-type method for studying synchronization problems," *Automatica*, vol. 13, no. 2, pp. 139–151, 1977.
27. R. Rüdenberg, *Elektrische Schaltvorgänge und verwandte Störungserscheinungen in Starkstromanlagen*. Julius Springer, Berlin, 1923.
28. ——, *Transient Performance of Electric Power Systems*. , McGraw-Hill, New York, 1950.

29. J. Schiffer, D. Zonetti, R. Ortega, A. Stankovic, T. Sezi, and J. Raisch, "A survey on modeling of microgrids–from fundamental physics to phasors and voltage sources," *Automatica*, vol. 74, pp. 135–150, 2016.
30. S. D. Umans, *Fitzgerald and Kingsley's Electric Machinery*. McGraw-Hill Higher Education, 2013.
31. A. van der Schaft, *L2-Gain and Passivity Techniques in Nonlinear Control*. Springer, 2000.
32. E. Venezian and G. Weiss, "A warning about the use of reduced models of synchronous generators," in *Science of Electrical Engineering (ICSEE), IEEE International Conference on the*. IEEE, 2016, pp. 1–5.
33. V. Venkatasubramanian, H. Schattler, and J. Zaborszky, "Fast time-varying phasor analysis in the balanced three-phase large electric power system," *IEEE Transactions on Automatic Control*, vol. 40, no. 11, pp. 1975–1982, 1995.
34. K. Visscher and S. De Haan, "Virtual synchronous machines for frequency stabilisation in future grids with a significant share of decentralized generation," in *SmartGrids for Distribution, 2008. IET-CIRED. CIRED Seminar*, june 2008, pp. 1 –4.
35. H. Wang and W. Du, *Analysis and Damping Control of Power System Low-frequency Oscillations*. Springer, 2016.
36. X. Wang, Y. Chen, G. Han, and C. Song, "Nonlinear dynamic analysis of a single-machine infinite-bus power system," *Applied Mathematical Modelling*, vol. 39, no. 10, pp. 2951–2961, 2015.
37. W. Winter, K. Elkington, G. Bareux, and J. Kostevc, "Pushing the limits: Europe's new grid: Innovative tools to combat transmission bottlenecks and reduced inertia," *IEEE Power and Energy Magazine*, vol. 13, no. 1, pp. 60–74, 2015.
38. V. A. Yakubovich, G. A. Leonov, and A. K. Gelig, *Stability of stationary sets in control systems with discontinuous nonlinearities*. World Scientific Singapore, 2004.
39. Q. Zhong and G. Weiss, "Synchronverters: Inverters that mimic synchronous generators," *IEEE Transactions on Industrial Electronics*, vol. 58, no. 4, pp. 1259 –1267, april 2011.